REVIEW OF AN ANALYTICAL MODEL FOR INDUCTION PLASMA COLUMNS IN LTE AND ATTEMPTS TO INCLUDE NONEQUILIBRIUM EFFECTS

Hans U. Eckert
3901 Via Pavion, Palos Verdes Estates, California 90274, U.S.A.

ABSTRACT

The energy balance equation for a thermal induction plasma column has been solved approximately by Bessel functions and applied to argon at ambient pressure. Good agreement with experimental data is obtained except near walls, where diffusion causes super LTE electron concentrations. The presence of the electric field in the skin zone also keeps the electron temperature above that of the heavy particles.

1. INTRODUCTION

The induction heating of flowing gases involves complex interaction between electromagnetic, fluid-and thermodynamic phenomena and rigorous treatment requires an elaborate computer program (1). In the absence of such a program and for fast, exploratory calculations, a simple model developed for one dimensional thermal induction columns (2,3,6), will be helpful. It accounts for moderate radiation losses and permits determination of field-and temperature distributions across the column, especially with argon at atmospheric pressure as plasma gas, for which the material has been charted. In the following the basic features of this model will be reviewed and the results compared with experimental data.

2. ANALYSIS

For an element of a plasma column in LTE the energy balance equation can be written

$$\frac{d^2S}{dr^2} + \frac{1}{r}\frac{dS}{dr} + \sigma E^2 - Q = 0 \qquad (1)$$

where $S \equiv \int_0^T \kappa dT$ is the heat conduction potential (κ = thermal conductivity), Q is the radiation source strength and the other symbols have their usual meaning.

The column is divided into two zones. In the external or dissipation zone Q may be disregarded against σE^2. For this zone Eq. (1) can be solved in closed form under the following two conditions: 1) the electrical conductivity σ is proportional to S

$$\sigma = c^2 S; \tag{2}$$

2) The variation of the induced electric field E over the column radius R follows a power law

$$E = E_R \left(\frac{r}{R}\right)^q, \tag{3}$$

where E_R is the value of E at r = R. With Eqs. (2) and (3) the solution of Eq. (1) for the external zone can be written:

$$S = A\, J_o\left[\lambda\left(\frac{r}{R}\right)^{q+1}\right] + B\, Y_o\left[\lambda\left(\frac{r}{R}\right)^{q+1}\right], \tag{4}$$

where A and B are integration constants, J_o and Y_o are the Bessel and Neumann functions of zero order and

$$\lambda \equiv \frac{cE_R R}{q+1} \tag{5}$$

is the eigenvalue of the system. Constant B can be eliminated by the boundary condition at r = R. In case $T_R = S_R = 0$, Eq. (4) reduces to

$$S = A \left| J_o\left[\lambda\left(\frac{r}{R}\right)^{q+1}\right] - \frac{J_o(\lambda)}{Y_o(\lambda)}\, Y_o\left[\lambda\left(\frac{r}{R}\right)^{q+1}\right] \right| \tag{6}$$

In the inner or radiation zone the increases with r in Q and σE^2 will approximately cancel out, so that

$$Q - \sigma E^2 \approx Q_o \tag{7}$$

where Q_o is the value of Q at r = 0. For this zone the solution of Eq. (1) is then

$$S = S_o + Q_o\left(\frac{r}{2}\right)^2 \tag{8}$$

To obtain a smooth distribution of S over the radius, Eqs. (6) and (8) must be matched at the zone interface. This procedure is described in Ref. (3).

3. RESULTS

a) Electron Diffusion

Temperature profiles obtained with the above model for argon induction plasmas at p = 1 atm. have been compared with exact numerical solutions of Eq. (1) by Pridmore-Brown (4) and with experimental data by Stokes (5). Fig. 1 shows the results for three different power inputs per unit column length.

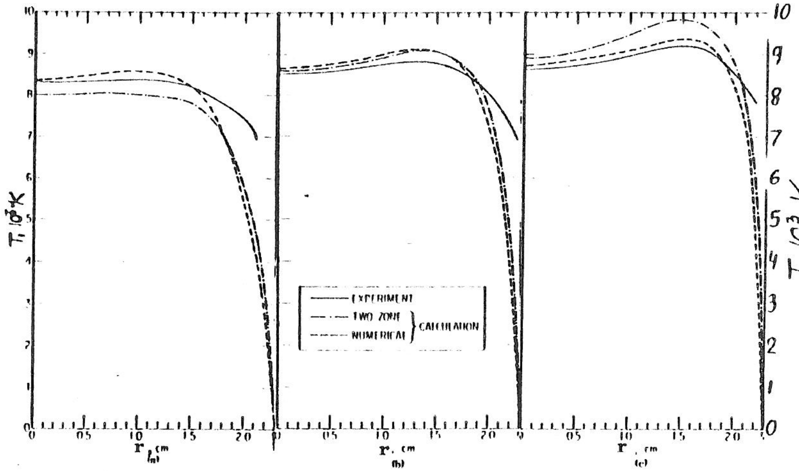

Fig 1. Measured and calculated temperature distributions across full-column argon induction plasmas at atmospheric pressure; f = 3.8 MHz. (a) P/L=250 W/cm. (b) P/L=500 W/cm. (c).... P/L=750 W/cm.

It is seen that the results of the two-zone model agree with the numerical calculations within a few percent. With the experiments agreement is also satisfactory, except near the wall, where the experiments indicate unrealistically high temperatures.

Stokes (5) has also measured temperature profiles for induction plasmas maintained in the annular space between coaxial cylinders, which are shown in Fig. 2 for two different power inputs. Here the effect of the two walls on the profiles is much more pronounced and agreement with the calculations exists only in a narrow region near the temperature maximum.

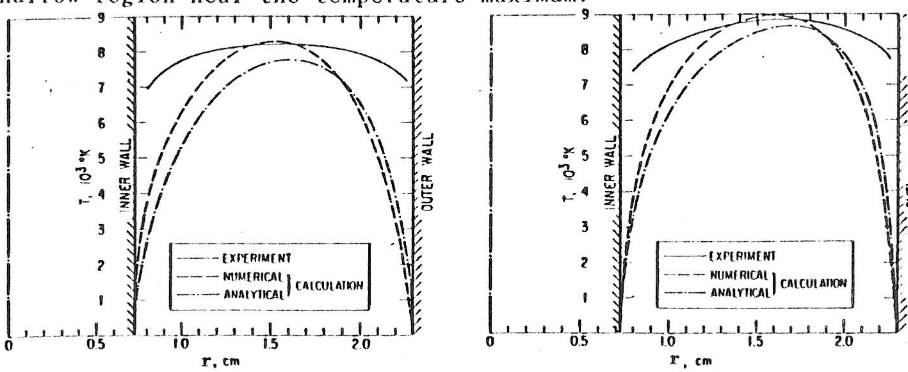

(a) (b)

Fig. 2. Measured and calculated temperature distributions in annular-column induction plasmas. f = 3.8 MHz, (a) P/L = 390 W/cm, (b) P/L = 620 W/cm.

The author has explained this discrepancy by ambipolar diffusion of electrons and positive ions to the walls (6), a process that is prevalent in low pressure glow discharges, but usually not considered in the treatment of thermal discharges. Since the electron density n_e is proportional to the electric conductivity σ, which according to Eq. (2) is proportional to S, the n_e-distribution should be proportional to that of S given by Eq. (6)

$$n_e = A' \left| J_o\left[\lambda\left(\frac{r}{R}\right)^{q+1}\right] - \frac{J_o(\lambda)}{Y_o(\lambda)} \; Y_o\left[\lambda\left(\frac{r}{R}\right)^{q+1}\right]\right| . \qquad (6')$$

To test this hypothesis and determine the constant A', it has been assumed that the plasma is in LTE at the location of the temperature maximum, so that here n_e is given by the Saha equation. To duplicate the experimental temperature profiles, the LTE temperatures corresponding to the n_e-profile of Eq. (6') have then been calculated from the Saha equation. The results are shown in Fig. 3. The agreement is seen to be very close in both cases, provided that the same exponent q, that had been obtained for the S-profile, is also used for the n_e-profile. If we set q=0, which corresponds to a uniform electric field and uniform electron temperature, the agreement is much poorer.

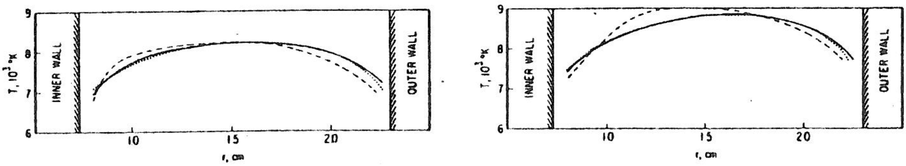

Fig. 3. Comparison of experimental temperatures from Fig. 2 with apparent LTE temperatures based on diffusion profile for electrons, Eq. (6'). Dashed lines: q=0; dotted lines: case (a) q=1.75 ; case (b) q=2.58 .

The close agreement indicates that a super LTE electron concentration builds up near walls and excessive temperatures are derived from spectroscopic data on LTE basis, especially, when the data represent absolute intensities, as in the case of Stokes.

In more recent work (7) the author has applied these results to calculate the variations in temperature and electron concentration along the axis of the carrier jet in an analytical induction torch (ICP), by assuming the jet to take on the role of the inner cylinder in the coaxial arrangement. The geometry of the torch considered has been described by Scott et al. (8). After emerging from the orifice at room temperature, the jet is exposed to the heat and electron fluxes from the surrounding plasma core. As a consequence, both, temperature and electron concentration rise, but the electron concentration rises much faster, than it would under LTE conditions. This is illustrated in Fig. 4 for a jet flow rate of 1 liter/min and an rf power input of 1 kW. In the observation zone, z >20 mm, the actual electron concentration $\bar{n}_e$ averaged over the jet area, exceeds the LTE concentration $n_e(\bar{T})$ by about an order of magnitude. Also shown are three experimental points obtained by Kalnicki et al. (9) for the same geometry and the same test conditions from Stark broadening of the hydrogen β-line, that is, independently of the existence of LTE. It is seen, that the results from the diffusion model are much closer to the experimental data than the LTE calculations. The existence of a super-LTE electron concentration in the carrier jet also explains the frequent observation that addition of an easily ionizable element, like Na, to the analyte solution has a much lower effect on the suppression of ion spectral lines in the ICP torch than in other excitation sources. In the ICP the electrons produced by ionization of Na have to compete with a large influx of electrons from the annular plasma.

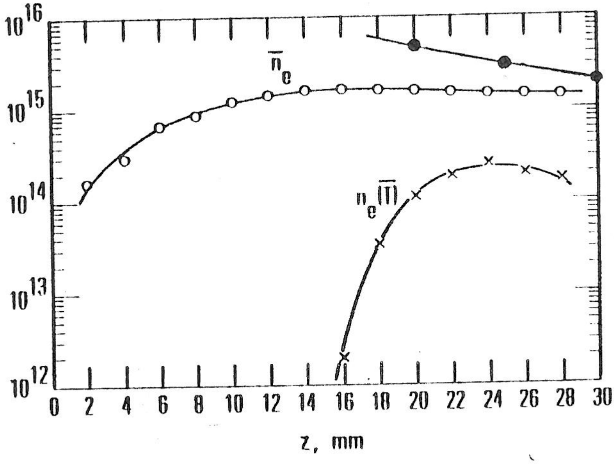

Fig. 4. Mean electron concentrations in ICP carrier jet vs. distance from orifice (7).

X ——— X Calculation based on LTE

0 ——— 0 Calculation based on diffusion model

● ——— ● Experimental data by Kalnicki (9) derived from Stark broadening of Hβ-line.

b) Two Temperature Plasma

In more accurate modeling of thermal induction plasmas one must account for the fact, that an electric field causes the temperature of the electrons, T_e, to exceed that of the heavy particles, T, because the energy from the field is first transmitted to the electrons, which in turn transfer it by collisions to the heavy particles. The energy balance equation (1) thus has to be split into two parts, one for the electrons and one for the heavy particles. Both equations are coupled by a collision term. For a rigorous treatment of two temperature plasmas, see Dresvin (10). In the following we want to show, how $T_e(r)$ can be determined in a first approximation from the two-zone model described in Section 2.

For the dissipation zone, which is the only zone of interest here, because E is significant (and $\sigma E^2 >> Q$), Dresvin's equations reduce to

a) for the electrons

$$\sigma E^2 = \frac{3}{2} k (T_e - T) \xi \nu n_e - \frac{1}{r} \frac{d}{dr} (\lambda_e r \frac{dT_e}{dr}), \qquad (1a)$$

b) for the heavy particles

$$\frac{3}{2} k (T_e - T) \xi \nu n_e = -\frac{1}{r} \frac{d}{dr} (\lambda_{ai} r \frac{dT}{dr}). \qquad (1b)$$

where ξ is the fraction of energy exchanged per collision, ν is the electron collision frequency, λ_e and λ_{ai} are the thermal conductivities of electrons and heavy particles, respectively.

According to Dresvin, the electron conduction term in Eq. (1a), is generally small and will be disregarded here, so that one obtains

$$T_e = T + \frac{\sigma E^2}{\frac{3}{2} k \xi \nu n_e} \qquad (9)$$

with $\sigma = \frac{n_e e^2}{m_e \nu}$ and $\xi \approx \xi_{el.} = \frac{2m_e}{M}$

where e and m_e are the electronic charge and mass, respectively, and M is the atomic mass, Eq. (9) can be written

$$T_e = T + \frac{M}{3k} \left(\frac{eE}{m_e \nu}\right)^2 \qquad (10)$$

It is noteworthy, that n_e does not appear in Eq. (10)

ν has been evaluated in Ref. (7) for argon at p = 1 atm. as a function of T_e and T. To obtain $T_e(r)$ from Eq. (10), T(r) has been determined from Eq. (6) and E(r) from Eq. (3).

A result from this calculation procedure is shown in Fig. 5, where T, T_e and E are plotted vs. r for a large argon-induction plasma (R = 7.75 cm, f = 2.6 MHz, P/L = 1270 W/cm). It is seen that only in the skin zone, where E >0.2 V/cm, does T_e differ significantly from T. In close proximity to the wall (r = 7.5 cm) T_e-T ≈ 2000K.

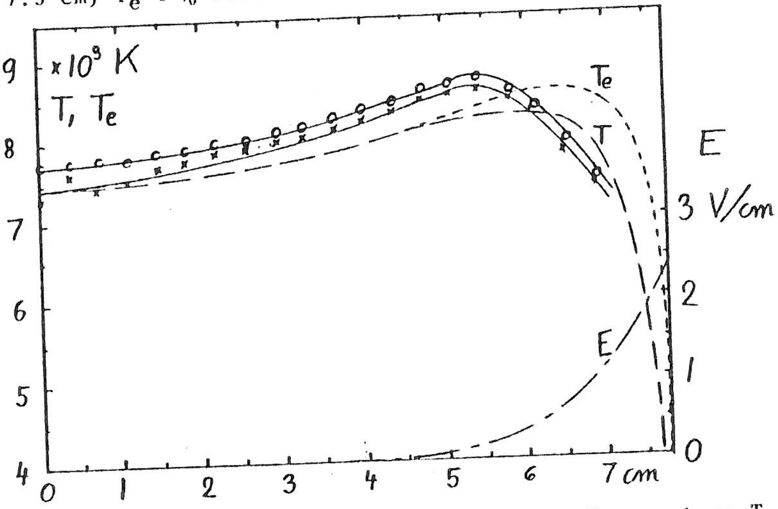

Fig. 5. Radial Distributions of Electron Temperature T_e, Plasma Temperature T, and Induced Electr. Field E in Argon Induction Plasma at P = 1 atm.
Calculations: .....T_e, — —,— T, — • — E. Experiments (11): X———X T_e from ArI 430 nm line, O———O T_e from continuum.

Also shown in Fig. 5 are spectroscopic determinations of T_e by Leonard (11). Agreement between the calculated and experimental data is good over 80% of the radius, but near the wall the calculated T_e-values are about 10% higher. A possible explanation for this discrepancy is, that the plasma was maintained in a swirl flow, which tended to keep a cool gas layer near the wall, a phenomenon not accounted for by the model.

Summarizing, it can be said that the above outlined simple model is adequate for describing thermal induction plasmas in which flow phenomena and two dimensional effects are not significant. Non LTE phenomena, caused by diffusion of electrons and by their incomplete energy exchange with heavy particles, can be approximately taken into account.

It may be added that recent extensive measurements by Barnes and Schleicher (12) of temperature profiles across ICP torches with and without central flow yield similar discrepancies with results from the authors own LTE computer model as the data show here, indicating effects of electron diffusion and/or-temperature. A computer program that accounts for these effects, has been proposed by Aeschbach (13).

REFERENCES

(1) M.I. Boulos, IEEE Trans. Plasma Sci. PS-4 28 (1976).

(2) H.U. Eckert, J. Appl. Phys. 41, 1520 (1970).

(3) H.U. Eckert, J. Appl. Phys. 41, 1529 (1970).

(4) H.U. Eckert and D.C. Pridmore Brown, J. Appl. Phys. 42, 5051 (1971).

(5) A.D. Stokes, International Conference on Gas Discharges London 1970, IEEE Publ. 70, 182.

(6) H.U. Eckert, J. Appl. Phys. 43, 46, (1972).

(7) H.U. Eckert, Proc. Interntl. Winter Conf. 1980 on Developments in Atomic Spectrochem. Analysis, San Juan Puerto Rico; Heiden & Son, Philadelphia, Penn. 1981.

(8) R.H. Scott, V.A. Fassel, R.N. Knisely and D.E. Nixon, Anal. Chem. 46, 75-80, (1974).

(9) D.J. Kalnicki, V.A. Fassel and R.N. Knisely, Appl. Spectrosc. 31, 137 (1977).

(10) S.V. Dresvin (editor), "Physics and Technology of Low Temperature Plasmas", Iowa State University Press 1977.

(11) S.L. Leonard, J. Quant. Spectrosc. Radiat. Transfer 12, 619 (1972).

(12) R.M. Barnes and R.G. Schleicher, Spectrochim. Acta 36B, 81, (1981).

(13) F. Aeschbach, ICP Information Newsletter 6, 272, (1980).